Fitting partial differential equations to space-time dynamics

Markus Bär, Rainer Hegger, and Holger Kantz
Max-Planck-Institut für Physik Komplexer Systeme, Nöthnitzer Strasse 38, D-01187 Dresden, Germany
(Received 24 June 1998)

The partial differential equations (PDEs) governing the dynamics of reaction-diffusion systems are reconstructed from data representing the spatially extended systems. The fitted equations are validated by a comparison of their numerical solutions and the input data and by computation of the isoclines of the fitted PDEs. [S1063-651X(99)02101-7]

PACS number(s): 05.45.Tp

Nonlinearities in equations of motion often result in complex dynamical behavior such as bifurcations under parameter variation and chaos. The experimental observation of such phenomena relies on the analysis of time series [1]. One of the most interesting goals of nonlinear time series analysis is the reconstruction of equations of motion based only on observed data. This issue is well studied for systems with a few active degrees of freedom. In pioneering works local linear models [2], global models consisting of radial basis functions [3], neural nets [4], and polynomials [5] have been successfully used to construct forecast maps. Since often only a single observable is recorded, these maps act on a reconstructed state space, usually the delay embedding space [6,7]. Once such a map is reconstructed from the observed data, it allows, e.g., for short time predictions and for the construction of new time series through iteration (bootstrapping), but also for the estimation of Lyapunov spectra [8]. Meanwhile there exists a well established knowledge about fitting model equations to maplike data, i.e., to data with a discrete time index.

In cases where all variables of physical interest are observed simultaneously, i.e., where the state space of the system is experimentally accessible, it makes sense to reconstruct ordinary differential equations (ODEs) underlying the dynamics. This has been done for many numerically simulated systems. For an example with experimental data from a driven nonlinear electric resonance circuit see Ref. [9]. In comparison to fitting forecast maps in the delay embedding space, fitting ODEs additionally contains the difficulty of determining temporal derivatives from data that are recorded with a given sampling rate and are contaminated with a certain amount of measurement noise. It is technically possible to fit ODEs also to noninvariate time series, but since chaotic motion requires (in the autonomous case) a scalar equation of at least third order in time, this is usually not considered as a reasonable physical approach.

A widely studied class of more complex systems are spatially extended nonequilibrium systems; their dynamics are routinely described by partial differential equations (PDEs). A lot of activity has focused on the emergence of spatiotemporal patterns [10]. These patterns are mostly periodic in space and stationary or periodic in time. Only recently, examples for spatiotemporal chaos have been discovered in convection experiments [11] and in chemical reactions [12,13]. Here we constrain ourselves to the study of reaction-diffusion processes that are often encountered in pattern forming chemical reactions [14] and biological systems [15]. Often models for these systems are only of qualitative nature due to the complexity of the processes involved and because of a lack of knowledge of the basic mechanisms. Thus it would be desirable to verify such models by extracting equations governing the dynamics in space and time from data. We restrict the analysis of this paper exclusively to numerically generated data, including a discussion on measurement noise. The purposes of this paper are to prove the feasibility of this goal and to stimulate similar analysis of experimental data. Estimates on the necessary spatial and temporal resolution of data are given. We chose three models with increasing complexity that are known to exhibit periodic waves as well as spatiotemporal chaos [16–20] and created data by numerical integration of these equations. The method requires either simultaneous measurement of all dynamical variables as in one-variable systems encountered in nonlinear optics [21] or reconstruction of the unmeasured quantities by additional assumptions about the dynamics (e.g., the validity of amplitude equations near the onset of an instability or symmetries between the variables as in the method of complex demodulation [22]). Under the constraint that all relevant variables are observed simultaneously, we address the problem of identifying PDEs from these data. In comparison to ODEs, additionally spatial derivatives have to be estimated and more independent terms potentially enter the equations. We do not want to conceal that these are more technical than conceptual problems. Fitting PDEs to spatiotemporal dynamics can have implications on the understanding of systems, in particular in order to obtain corrections to model equations that are derived involving approximations and heuristic arguments and in order to fix parameters in model equations.

We model the unknown PDEs as polynomials of the independent variables. In the case of a two-component field in one space dimension these variables are the field $\vec{u}=(u,v)$ itself and its spatial derivatives, denoted by u_x, v_x, u_{xx}, etc., in the following. We want to derive expressions $\dot{u}=f(u,v,u_x,v_x,u_{xx},v_{xx}\ldots)$ and $\dot{v}=g(u,v,u_x,v_x,u_{xx},v_{xx},\ldots)$. For f and g we choose multivariate polynomials of sufficiently high order that can be considered as Taylor expansions of the unknown nonlinear functions. For a recent approach to this problem using a different method see Ref. [23].

We assume that the data are taken with a spacing η in space and δ in time, $u_{n,i}=u(t=n\delta,x=i\eta)$. The data set can

consist of either a few successive snapshots or a long series of multichannel measurements at neighboring sites. How many successive images or how many adjacent positions have to be measured depends on the order of the highest derivatives and on the desired accuracy. Approximations of the derivatives in different order are possible. Additional filtering can be used to suppress noise. Suitable estimators and the influence of noise are described in the last part of this paper. Due to the minimum of three independent observations for symmetric derivative estimators of the first and second derivatives, we need either at least three successive snapshots or a time series of three neighboring spatial positions if we assume that no higher than second derivatives occur.

For the determination of f we solve the minimization problem

$$\sigma^2=\sum_{\{i,n\}}\left(u_{t;n,i}-\sum c_{jklmop}u_{n,i}^{j}v_{n,i}^{k}\times u_{x;n,i}^{l}v_{x;n,i}^{m}u_{xx;n,i}^{o}v_{xx;n,i}^{p}\right)^2\stackrel{!}{=}\min \tag{1}$$

with respect to the parameters c_{jklmop} (a corresponding problem is solved independently for g). The first sum extends over a reasonably large set of tuples $(u_{t;n,i},u_{n,i},v_{n,i},u_{x;n,i},v_{x;n,i},u_{xx;n,i},v_{xx;n,i})$. In order to keep the number of fit parameters $c\ldots$ small, we consider only a physically meaningful set of terms in the polynomial, e.g., we choose a highest power in u and v, consider only even powers of u_x and v_x of the spatiotemporal patterns, and exclude combinations of first and second derivatives because of symmetry properties $(x\rightarrow -x)$. The minimization requires one to solve a set of coupled linear equations by matrix inversion or, if many parameters are involved, employing singular value decomposition. Since this can be done extremely fast, we explicitly look for the best of all possible combinations of a subset of these terms. When the number of terms does not exceed 20, we can compare all possible combinations, whereas for more terms, we employ a backward elimination scheme. We perform a fit including all terms, then search for the term that when being excluded leads to the smallest increase of the error, and thus reduce step by step the model. When we speak here and in the following about the error we mean the value of σ from Eq. (1) at the minimum, normalized to the standard deviation of the temporal derivative.

As a first example, we treat a model recently suggested to capture dynamics of an extended system near a codimension-2 bifurcation (Takens-Bogdanov-point) [16],

$$\frac{\partial u}{\partial t}=v,\qquad \frac{\partial v}{\partial t}=(\mu-u^2)v-u-au^2-u^3+\frac{\partial^2 u}{\partial x^2}+\kappa\frac{\partial^2 v}{\partial x^2}, \tag{2}$$

with $\mu=1/5$, $a=2.08$, and $\kappa=1$. A random initial condition was numerically integrated with time steps that were more than a factor 10 finer than the sampling of the data used for the fits. For the numerical solution of these equations and the other examples that follow, periodic boundary conditions are employed and simple explicit Euler schemes are used. The spatial and temporal discretization have been checked for convergence. Spatiotemporal patterns created by Eq. (2) resemble the pattern in Fig. 1.

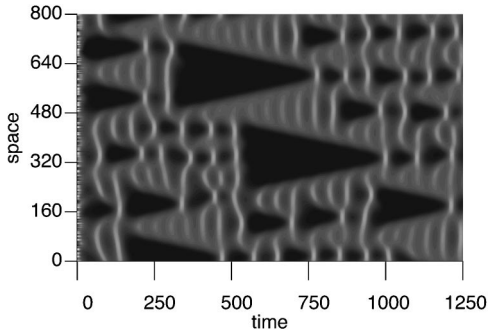

FIG. 1. Typical spatiotemporal pattern (u component) of the PDE fitted to data from Eq. (2) starting from random initial conditions. The parameters are $a=2.08$, $\mu=0.2$, and $\kappa=1.0$, the system length is 100, and the integration time 78.32. All units are dimensionless.

For the fit of the PDE we compile a list of about 20 combinations of powers of u, v, u_x, v_x, u_{xx}, and v_{xx} and look for the best of all combinations of subsets of them. The minimum value of Eq. (1) as a function of the subset size n decreases in n and saturates at an error around 1% when seven terms are included in the expression for g and only a single term is used for f. These terms are in fact those of Eq. (2) above. The nullclines of these fitted equations are in perfect agreement with those of Eq. (2) in those regions of the u-v plane that are represented by the input data. Outside this area, the nullclines of the fit cannot be expected to be identical to those of the original system, although in this special case they are (see below). As a final check of the model, we take a random initial condition and integrate the fitted PDE. The spatiotemporal patterns generated by the fitted equations are shown in Fig. 1. They are qualitatively indistinguishable from patterns generated by the original PDE.

Since we fitted noise free data generated by a PDE with polynomials on the right-hand side by polynomials, it is not surprising that the resulting PDE is of the same structure as Eq. (2) with almost exactly the correct coefficients, such that it passes the test for model validation. Due to the fact that $\dot{u}=v$, we could here rely on the sole measurement of the u-field component and fit a PDE of second order in time. This approach is in fact similarly successful.

The good results reported for model (2) can be rationalized from the fact that the functions f and g are polynomials

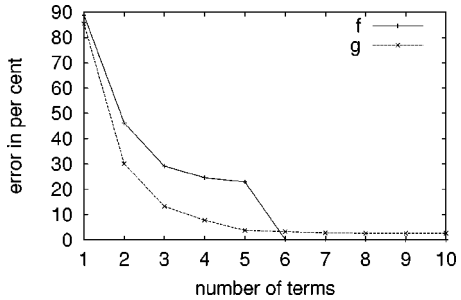

FIG. 2. Minimum error of the optimal polynomial consisting of n out of 22 terms in the polynomial ansatz for f and g of the model (3). The parameters used are $\epsilon=0.15$, $a=0.84$, and $b=0.20$.

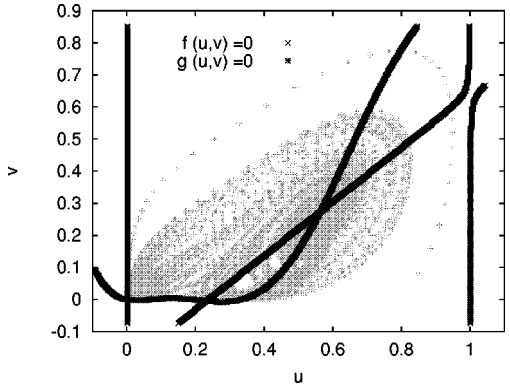

FIG. 3. Nullclines of the PDE fitted to time series data from Eq. (3), to be compared to Eq. (3). The projections of the input data into the u-v plane are shown in gray. The parameters are the same as in Fig. 2.

themselves. Therefore, we study a simplified model of CO oxidation on Pt(110)[17] where this is not the case:

$$\frac{\partial u}{\partial t} = -\frac{1}{\epsilon}u(u-1)\left(u-\frac{b+v}{a}\right)+\frac{\partial^2 u}{\partial x^2},$$

$$\frac{\partial v}{\partial t} = h(u)-v, \tag{3}$$

$$h(u)=\begin{cases} 0, & 0\leqslant u<1/3 \\ 1-6.75u(u-1)^2, & 1/3\leqslant u\leqslant 1 \\ 1, & 1<u. \end{cases}$$

Again we compare all possible models based on selections out of 22 terms. The saturation of the error as a function of the number of terms n is shown in Fig. 2. Whereas there exists a clear signature for the u equation [and we find exactly the six terms in Eq. (3)], there is a smooth transition for the v equation. The polynomial can reproduce the piecewise defined function h better with more terms included. For a model consisting of ten terms we repeat the analysis for model validation: nullclines (Fig. 3) and numerical integration (Fig. 4). Since here the fitted PDE is of a different structure than the original one (global polynomial versus piecewise polynomial) we show in Fig. 4 a comparison of model and fit.

The functions f and g can be determined only in ranges of their arguments that are sampled by the data. Therefore, this approach can be successful only for aperiodic data with spatiotemporal disorder or for transient motion. If, on the contrary, only a single periodic orbit is observed, this is thus insufficient to fix f and g at least as soon as the ansatz chosen for the fit is not of exactly the form of the true model equation. In general, there is an extended region in parameter space where spatiotemporal chaos is observed. Thus it is possible to study also the parameter dependence of the fitted model equations. In a similar fashion, one can explore the domain where periodic patterns are observed by employing suitable perturbations or forcing to the system. Here we will restrict ourselves to model verification for selected parameter values.

The experimental measurement of transient spatiotemporal dynamics caused by external perturbations is a possible cure in systems where the final patterns exhibit periodic or stationary temporal dynamics (for an experimental example in a chemical reaction perturbed by laser illumination see Ref. [24]). We simulate numerically such a transient for Eq. (3) (with slightly different parameters, where stable periodic solutions exist) by subsequently shortening the system size and consequently the wavelength of the pattern during integration. Performing the minimization for these transient data leads to the nullclines shown in Fig. 5, where also the transient solution is shown in gray. Due to the fact that this particular solution covers a considerable part of the u-v plane, we can again successfully determine the dynamics.

As a third and considerably more complicated example we have studied data generated from a model of the catalytic NO reduction with CO on Pt suggested by Imbihl and coworkers [18,19]:

$$\frac{\partial u}{\partial t} = k_1 p_{\mathrm{CO}}(1-u-v)-k_2(u,v)u-k_3uw+\frac{\partial^2 u}{\partial x^2},$$

$$\frac{\partial v}{\partial t} = k_1 p_{\mathrm{NO}}(1-u-v)-k_4(u,v)v-k_5 v f(u+v,w)+\frac{\partial^2 v}{\partial x^2}, \tag{4}$$

$$\frac{\partial w}{\partial t} = k_5 v f(u+v,w)-k_3uw.$$

The equations describe the dynamics of the concentrations of CO (u), NO (v) and O (w) on the surface. The control parameters are the partial pressures p_{CO} and p_{NO} and the

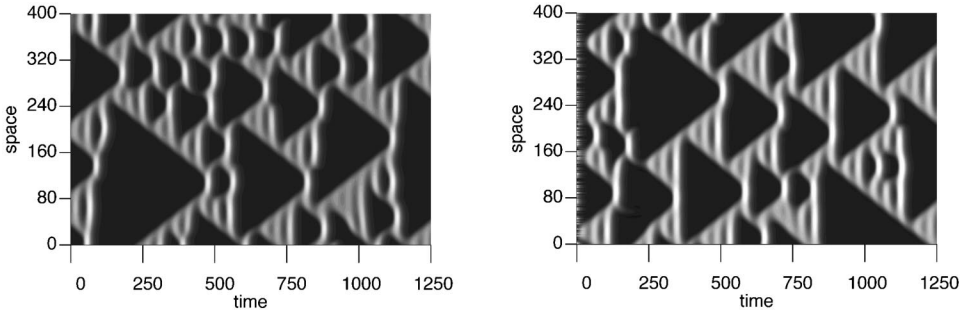

FIG. 4. Typical spatiotemporal patterns (v component) of Eq. (3) (left) and of the PDE fitted to data from Eq. (3) (right), starting from random initial conditions. The parameters are the same as in Fig. 2. The system length is 50 and the integration time shown is 122.37, both in dimensionless units.

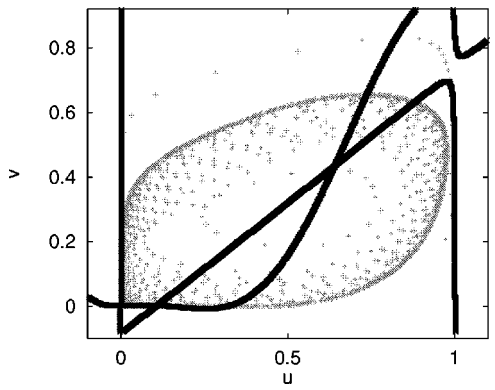

FIG. 5. Nullclines of the fitted PDE obtained from the almost periodic data shown in gray, to be compared to Eq. (3). The parameters are $\epsilon=0.05$, $a=0.84$, and $b=0.1$.

catalyst temperature T that enters via Arrhenius-like terms into the desorption rate constants k_2 and k_4, the reaction rate of CO oxidation k_3, and the rate of NO dissociation k_5. The desorption rates of NO and CO also contain an exponential dependence on the coverage of CO and NO, namely,

$$k_{2,4}=\nu_{2,4}\exp\{-[E_{\mathrm{ad}}^{\mathrm{CO,NO}}-k_6(u+v)^2]/k_BT\}. \qquad (5)$$

This dependence is crucial for the occurrence of dynamic instability and has been termed surface explosion, since an increase in the coverage leads to a very rapid increase in desorption of NO and CO [19]. The function $f(u+v,w)$ indicates the amount of empty surface sites and has the empirically determined form $f(u+v,w)=\max[1-(u+v)/0.61-w/0.4,0]$ [19]. The dynamics of reaction-diffusion waves in this model has been investigated recently by Christoph [20]. He found that the model exhibits stable pulses at low p_{CO}, which upon an increase of p_{CO} develop modulations and finally lead to complex periodic patterns with spontaneous creation of excitation pulses. We have generated data in the complex periodic regime in parameter space subject to constant external perturbations that lead to transient spatiotemporally chaotic motion.

Because we have to deal with more independent variables and the exponential term requires a polynomial of higher order for a reasonable fit, we compose the right-hand side of the PDE of about 100 terms, which are then reduced by backward elimination. Thus we perform a first fit with all terms included and then eliminate term by term, each step skipping the term whose omission leads to the least increase of the error. We find reasonable errors of about 2% with models as small as about 20 terms (see Fig. 6).

Since data from this model fill the three-dimensional phase space (u, v, w) only sparsely, the equations of motion thus obtained are valid only in close vicinity to the observed data (on the ''attractor''), whereas outside they are considerably wrong (in particular, due to the polynomial structure of our fit, the fitted functions diverge for large arguments). Therefore, we cannot present a reasonable comparison between the nullclines of the fitted PDE and of Eq. (4). Under iteration, however, the fitted equations are stable and yield periodic space-time patterns that are qualitatively the same as those of Eq. (4) reported in Ref. [20] (Fig. 7), when we choose a spatial pattern from Eq. (4) as an initial condition.

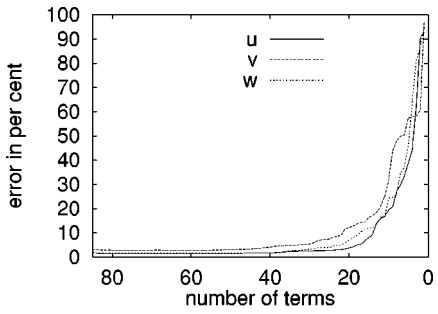

FIG. 6. Increase of the errors when applying the backward elimination technique to obtain the best model with n terms for data from Eq. (4). The parameters used in Eq. (4) are $p_{\mathrm{CO}}=8.5\times10^{-7}$mbar, $p_{\mathrm{NO}}=9.25\times10^{-7}$mbar, and $T=424$ K. The diffusion constants of CO and NO are set to 1 [see Eq. (4)].

Starting from random initial conditions, the integration leads to diverging solutions since such an initial condition is generally too far from the attractor and thus outside the range in phase space where we can expect the fitted equations to be valid.

It has been suggested to eliminate one variable of Eq. (4) adiabatically. Fitting PDEs of only two variables to the time evolution of different components of the field, we can in fact confirm that the dynamics of the u variable is well determined by only the u and v fields (2% error), but that the v dynamics is less well determined by that at least with a polynomial ansatz (about 7% error), and that, finally, the w dynamics is badly predicted by v and w (13% error) and even worse by u and w (19% error). Thus an adiabatic elimination of w seems possible when accepting some error.

We want to conclude with a discussion of a crucial aspect, namely, the estimation of the temporal and spatial derivatives. Apart from being sufficiently noise free, measurements have to be performed with sufficient temporal and spatial resolution. The simplest (symmetric) estimators are exact in order δ^2 and η^2, respectively:

$$u_{t;n,i}=\frac{1}{2\delta}(u_{n+1,i}-u_{n-1,i}),$$

$$u_{x;n,i}=\frac{1}{2\eta}(u_{n,i+1}-u_{n,i-1}), \qquad (6)$$

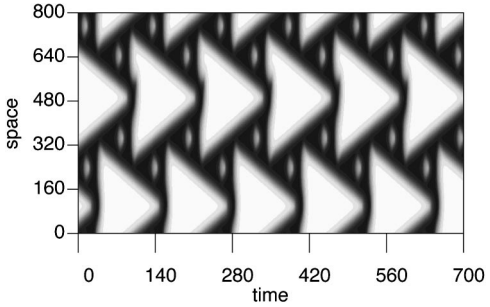

FIG. 7. Spatiotemporal pattern created by the polynomial PDE fitted to data from Eq. (4) (u field). The parameters are the same as in Fig. 6. The system length and the time are given in dimensionless units obtained by a proper scaling of Eq. (4). In rescaled physical units the time of integration shown corresponds to approximately 980 s and the length shown is 2 mm.

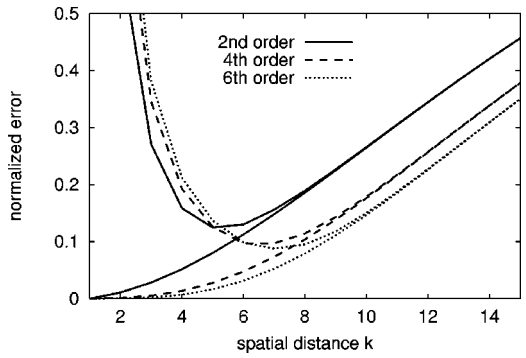

FIG. 8. Errors of the estimated second derivatives u_{xx} for the pattern of Fig. 1 as a function of the spatial resolution (distance k of the given sampling) for noise free data (converging towards zero for small k) and data with measurement noise (large errors at small k). For large k (low spatial resolution) the systematic errors are dominant.

$$u_{xx;n,i}=\frac{1}{\eta^2}(u_{n,i+1}+u_{n,i-1}-2u_{n,i}),$$

and for v correspondingly. One can easily use estimators of fourth or sixth order where, however, five or seven successive images or neighboring time series are required. For rough samplings the use of higher-order estimators is advantageous, as well as for noise contamination. In Fig. 8 we show the average error when estimating the second spatial derivatives u_{xx} from the pattern shown in Fig. 1, as a function of the spatial resolution [replacing, e.g., $i\pm1$ by $i\pm k$ in Eq. (6)], for noise free data and data with 0.5% white measurement noise. The three line types represent Taylor estimators of second, fourth, and sixth order. For high spatial resolution and thus high degeneracy of the variables entering the differences, noise introduces large errors, whereas bad resolution (large k) introduces large systematic errors but almost eliminates the errors due to noise. On a noise-level-dependent intermediate k the total error is lowest, where the higher-order estimators are superior. The situation is similar for first order derivatives, but errors due to noise are much smaller. The use of Savitzky-Golay filters [25] can reduce errors due to noise by about one-third, but noise remains a crucial problem. Nonlinear noise reduction techniques may help [26]. As for the required spatial resolution, in typical reaction-diffusion systems, the length scale on which concentrations change considerably lies between millimeters for reactions in solution and micrometers for surface reactions and biological systems. Sampling a grid in space with these resolutions is possible with experimental techniques and thus sufficient for a determination of the spatial derivatives.

To conclude, we have shown that one can successfully model PDEs from data if the relevant components of the fields are experimentally observed. Our polynomial approach can be replaced by other nonlinear functions, where it is advantageous when the fit parameters are contained linearly (which is not the case for neural nets).

Space and time in PDEs can be rescaled independently. If for simplicity δ and η are set to unity, the integration of the resulting PDE reproduces the observed data when sampled in the same way. Independent of this, the nullclines of the fitted equations represent the nullclines of the system, without using information about the sampling in space and time. The variables u and v can be rescaled and shifted and in experiments are rescaled and shifted in order to exploit the full ranges of analog-to-digital converters. Altogether this leads to the phenomenon that every single PDE is representative of a whole family of equations. This has to be taken into account when PDEs fitted to experimental data and model equations are to be compared. An unknown offset in the variables makes the situation quite complicated since under a shift of u or v even new combinations of powers may occur. The best strategy is thus to use all these operations to reduce the number of terms and to replace as many as possible nontrivial coefficients by unity.

The fitting of PDEs with polynomials has been tested for reaction-diffusion–type models. Thus only first and second derivatives have been included in the ansatz. Some pattern forming systems are governed by spatially nonlocal coupling terms, e.g., in nonlinear optics [21] and electrochemistry [27]. Models of these systems contain either integral terms or derivatives in exponentials. Both types of coupling terms can be expanded in Taylor series of the local derivatives (see, e.g., Ref. [15], Chap. 9). Thus an extended polynomial approach is also applicable to these systems. Moreover, the fitting approach introduced can be used to estimate the quality of reduced models such as amplitude equations (for an example see Refs. [28] and [29]). The method is useful in cases where all observables are known, but no information can be given on the physical model. It is suitable especially for dynamical systems with high attractor dimension (spatiotemporal chaos). Thus it supplements model reduction approaches using Galerkin projections or empirical eigenfunctions [30], which are often used to reconstruct spatiotemporal dynamics if the attractor has only a few degrees of dynamical freedom.

We are grateful to Jan Christoph and Markus Eiswirth for communicating their unpublished results on the NO-CO model [see Eq. (4)].

[1] H. Kantz and T. Schreiber, *Nonlinear Time Series Analysis* (Cambridge University Press, Cambridge, 1997).

[2] J. D. Farmer and J. J. Sidorowich, Phys. Rev. Lett. **59**, 845 (1987).

[3] D. S. Broomhead and D. Lowe, Complex Syst. **2**, 321 (1988).

[4] A. Lapedes and R. M. Farber, Los Alamos Technical Report No. LA-UR 2662, 1987 (unpublished).

[5] H. D. I. Abarbanel, R. Brown, and J. B. Kadtke, Phys. Rev. A **41**, 1782 (1990).

[6] F. Takens, in *Dynamical Systems and Turbulence*, edited by D. Rand and L.-S. Young, Lecture Notes in Mathematics Vol. 898 (Springer, Heidelberg, 1981).

[7] T. Sauer, J. A. Yorke, and M. Casdagli, J. Stat. Phys. **65**, 579 (1991).

[8] M. Sano and Y. Sawada, Phys. Rev. Lett. **55**, 1082 (1985).
[9] R. Hegger, H. Kantz, F. Schmüser, M. Diestelhorst, R. P. Kapsch, and H. Beige, CHAOS **8**, 727 (1998).
[10] M. C. Cross and P. C. Hohenberg, Rev. Mod. Phys. **65**, 851 (1993).
[11] M. C. Cross and P. C. Hohenberg, Science **263**, 1569 (1994).
[12] S. Jakubith, H. H. Rotermund, W. Engel, A. von Oertzen, and G. Ertl, Phys. Rev. Lett. **65**, 3013 (1990).
[13] Q. Ouyang and J. M. Flesselles, Nature (London) **379**, 143 (1996).
[14] R. Kapral and K. Showalter, *Chemical Waves and Patterns* (Kluwer, Dordrecht, 1995).
[15] J. D. Murray, *Mathematical Biology* (Springer, Berlin, 1989).
[16] M. Argentina and P. Coullet, Phys. Rev. E **56**, R2359 (1997).
[17] M. Bär, N. Gottschalk, M. Eiswirth, and G. Ertl, J. Chem. Phys. **100**, 1202 (1994); M. Bär and M. Eiswirth, Phys. Rev. E **48**, R1635 (1993).
[18] J. Evans, H. H. Madden, and R. Imbihl, J. Chem. Phys. **96**, 4805 (1992).
[19] R. Imbihl, T. Fink, and K. Krischer, J. Chem. Phys. **96**, 6236 (1992).
[20] J. Christoph (unpublished); J. Christoph and M. Eiswirth (unpublished).
[21] R. Neubecker, G.-L. Oppo, B. Thuering, and T. Tschudi, Phys. Rev. A **52**, 791 (1995).
[22] P. Kolodner, S. Slimani, and N. Aubry, Physica D **85**, 165 (1995); H. Voss, PhD. thesis, Universität Potsdam, 1998 (unpublished).
[23] H. Voss, M. Bünner, and M. Abel, Phys. Rev. E **57**, 2820 (1998).
[24] O. Steinbock and S. C. Müller, Physica A **188**, 61 (1992).
[25] W. H. Press, B. P. Flannery, S. A. Teukolsky, and W. T. Vetterling, *Numerical Recipes* (Cambridge University Press, Cambridge, 1992).
[26] H. Kantz, T. Schreiber, I. Hoffmann, T. Buzug, G. Pfister, L. G. Flepp, J. Simonet, R. Badii, and E. Brun, Phys. Rev. E **48**, 1529 (1993).
[27] N. Mazouz, G. Flätgen, and K. Krischer, Phys. Rev. E **55**, 2260 (1997).
[28] J. M. Fullano, P. LeGal, M. Rossi, and S. Zaleski, Physica D **102**, 37 (1997).
[29] D. P. Vallette, G. Jacobs, and J. P. Gollub, Phys. Rev. E **55**, 4274 (1997).
[30] P. Holmes, J. L. Lumley, and G. Berkooz, *sc Turbulence, Coherent Structures, Dynamical Systems and Turbulence* (Cambridge University, Cambridge, 1996).